Inorg. Chem. **2006**, *45*, 2669–2677

Ten-Vertex Iron–Monocarbollide Complexes: Synthesis and Reactivity of the Anion [4,9-{Fe(CO)$_4$}-9,9,9-(CO)$_3$-*arachno*-9,6-FeCB$_8$H$_{11}$]$^-$

Andreas Franken, Thomas D. McGrath, and F. Gordon A. Stone*

Department of Chemistry and Biochemistry, Baylor University Waco, Texas 76798-7348

Received November 10, 2005

The reagent [*arachno*-4-CB$_8$H$_{14}$] reacts with [Fe$_3$(CO)$_{12}$] in tetrahydrofuran (THF) at reflux temperatures, followed by addition of [N(PPh$_3$)$_2$]Cl, to afford [N(PPh$_3$)$_2$][4,9-{Fe(CO)$_4$}-9,9,9-(CO)$_3$-*arachno*-9,6-FeCB$_8$H$_{11}$] (**3**). In the anion of **3**, one iron atom is part of the open CBBFeBB face of a 10-vertex {*arachno*-9,6-FeCB$_8$} cage, to which the second iron atom is attached via an Fe–Fe bond and an additional exo-polyhedral Fe–B σ bond. Upon heating **3** in refluxing toluene, the closed 10-vertex species [N(PPh$_3$)$_2$][2,2,2-(CO)$_3$-*closo*-2,1-FeCB$_8$H$_9$] (**4**) is obtained, whereas the isomeric compound [N(PPh$_3$)$_2$][6,6,6-(CO)$_3$-*closo*-6,1-FeCB$_8$H$_9$] (**5**) is isolated upon heating [*closo*-4-CB$_8$H$_9$]$^-$ and [Fe$_3$(CO)$_{12}$] in refluxing THF with subsequent addition of [N(PPh$_3$)$_2$]Cl. Protonation of **3** using CF$_3$SO$_3$H in CH$_2$Cl$_2$ gives the charge-compensated compound [4,9-{Fe(CO)$_4$}-4-(μ-H)-9,9,9-(CO)$_3$-*arachno*-9,6-FeCB$_8$H$_{11}$] (**6**), in which the B–Fe σ bond of the precursor has been converted to a B–H $\rightharpoonup$ Fe linkage. In contrast, **3** with {M(PPh$_3$)}$^+$ gives the trimetallic species [1,3,4,9-{MFe(CO)$_4$(PPh$_3$)}-1,3-(μ-H)$_2$-9,9,9-(CO)$_3$-*arachno*-9,6-FeCB$_8$H$_9$] (M = Cu (**7**), Ag (**8**)) in which the three metal centers form a V-shaped M–Fe–Fe unit. Compound **6** reacts with PEt$_3$ in the presence of Me$_3$NO to yield [4,9-(PEt$_3$)$_2$-9,9-(CO)$_2$-*nido*-9,6-FeCB$_8$H$_{10}$] (**9**). In the latter, the formerly exo-polyhedral {Fe(CO)$_4$} fragment has been replaced by a PEt$_3$ ligand, with a second PEt$_3$ substituting one CO group at the remaining cluster iron vertex. The novel structural features of compounds **3**–**9** have been confirmed by single-crystal X-ray diffraction studies.

Introduction

We have for some years been investigating the chemistry of metal−monocarbollide species[1,2] in an attempt to redress a perceived imbalance between reports of these compounds in the literature relative to their much more well-studied dicarbollide counterparts.[3] However, until recently, our studies have essentially been limited to icosahedral {MCB$_{10}$} clusters,[1,2] a consequence of the difficulty of access to monocarboranes smaller than the {CB$_{10}$} system.[4] The discovery of the so-called Brellochs reaction,[5] as well as its subsequent elaboration,[6−8] has allowed intermediate-sized monocarboranes to be synthesized readily and in good yields from commercially available decaborane (B$_{10}$H$_{14}$). As a consequence, metallacarborane chemists are presented with a "golden opportunity". Sub-icosahedral metal−monocarbollide complexes in principle are now within reach via the many smaller carboranes that are newly accessible. In expanding our studies in this direction, we have reported 11-vertex {MCB$_9$} clusters (M = Re,[9] Mn,[10] Mo[11]) synthe-

(1) McGrath, T. D.; Stone, F. G. A. *J. Organomet. Chem.* **2004**, *689*, 3891.
(2) McGrath, T. D.; Stone, F. G. A. *Adv. Organomet. Chem.* **2005**, *53*, 1.
(3) Grimes, R. N. In *Comprehensive Organometallic Chemistry*; Wilkinson, G., Abel, E. W., Stone, F. G. A., Eds.; Pergamon Press: Oxford, U.K., 1982; Vol. 1, Section 5.5. Grimes, R. N. In *Comprehensive Organometallic Chemistry II*; Abel, E. W., Stone, F. G. A., Wilkinson, G., Eds.; Pergamon Press: Oxford, U.K., 1995; Vol. 1, Chapter 9. Grimes, R. N. *Coord. Chem. Rev.* **2000**, *200*−*202*, 773.
(4) Stíbr, B. *Chem. Rev.* **1992**, *92*, 225.
(5) Brellochs, B. In *Contemporary Boron Chemistry*; Davidson, M. G., Hughes, A. K., Marder, T. B., Wade, K., Eds.; Royal Society of Chemistry: Cambridge, U.K., 2000; p 212.
(6) Stíbr, B. *Pure Appl. Chem.* **2003**, *75*, 1295.
(7) Franken, A.; Kilner, C. A.; Thornton-Pett, M.; Kennedy, J. D. *Collect. Czech. Chem. Commun.* **2002**, *67*, 869. Jelínek, T.; Thornton-Pett, M.; Kennedy, J. D. *Collect. Czech. Chem. Commun.* **2002**, *67*, 1035.
(8) Brellochs, B.; Backovsky, J.; Stíbr, B.; Jelínek, T.; Holub, J.; Bakardjiev, M.; Hnyk, D.; Hofmann, M.; Císarová, I.; Wrackmeyer, B. *Eur. J. Inorg. Chem.* **2004**, 3605.
(9) Du, S.; Kautz, J. A.; McGrath, T. D.; Stone, F. G. A. *Organometallics* **2003**, *22*, 2842.
(10) (a) Du, S.; Farley, R. D.; Harvey, J. N.; Jeffery, J. C.; Kautz, J. A.; Maher, J. P.; McGrath, T. D.; Murphy, D. M.; Riis-Johannessen, T.; Stone, F. G. A. *Chem. Commun.* **2003**, 1846. (b) Du, S.; Jeffery, J. C.; Kautz, J. A.; Lu, X. L.; McGrath, T. D.; Miller, T. A.; Riis-Johannessen, T.; Stone, F. G. A. *Inorg. Chem.* **2005**, *44*, 2815.
(11) Lei, P.; McGrath, T. D.; Stone, F. G. A. *Chem. Commun.* **2005**, 3706.

10.1021/ic051946i CCC: $33.50
Published on Web 01/24/2006

Chart 1

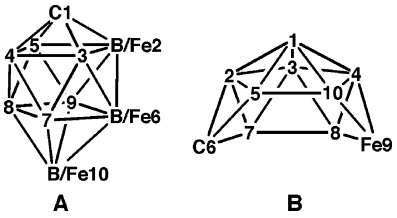

sized from [6-Ph-*nido*-6-CB_9H_{11}]$^-$ and more recently a pair of 9- and 10-vertex ferracarboranes prepared from [*closo*-1-CB_7H_8]$^-$.[12] Following on from the latter, we have performed a comparative study upon 10-vertex ferracarboranes derived from {CB_8} precursors, the results of which we now present. (Vertex numbering in the 10-vertex (**A**) *closo*-$FeCB_8$, and (**B**) *nido*- or *arachno*-$FeCB_8$, cages discussed herein is shown in Chart 1.)

Results and Discussion

We have recently prepared the salts [$N(PPh_3)_2$][7,7,7-$(CO)_3$-*closo*-7,1-$FeCB_7H_8$] (**1**) and [$N(PPh_3)_2$][6,6,6,10,10,-10-$(CO)_6$-*closo*-6,10,1-$Fe_2CB_7H_8$] (**2**) by heating [NBu^n_4]-[*closo*-1-CB_7H_8] with [$Fe_3(CO)_{12}$] in THF followed by addition of [$N(PPh_3)_2$]Cl (Chart 2).[12] Using a similar methodology, we obtained [$N(PPh_3)_2$][4,9-{$Fe(CO)_4$}-9,9,9-$(CO)_3$-*arachno*-9,6-$FeCB_8H_{11}$] (**3**) from [*arachno*-4-CB_8H_{14}] with [$Fe_3(CO)_{12}$] in THF at reflux temperatures followed by addition of [$N(PPh_3)_2$]Cl. An X-ray diffraction study upon the product was required to establish definitively its molecular structure. One of the three crystallographically independent anions of **3** is presented in Figure 1. Two iron atoms are present and are connected via an Fe−Fe bond (Fe(1A)−Fe(2A) = 2.7033(6) Å), with one of them a vertex in the *arachno*-10-vertex cluster system, and the other bonded exopolyhedrally to the cage via a direct Fe−B σ bond (Fe(1A)−B(4A) = 1.996(3) Å). Both iron centers possess pseudo-octahedral coordination spheres and are formally in the +2 oxidation state.

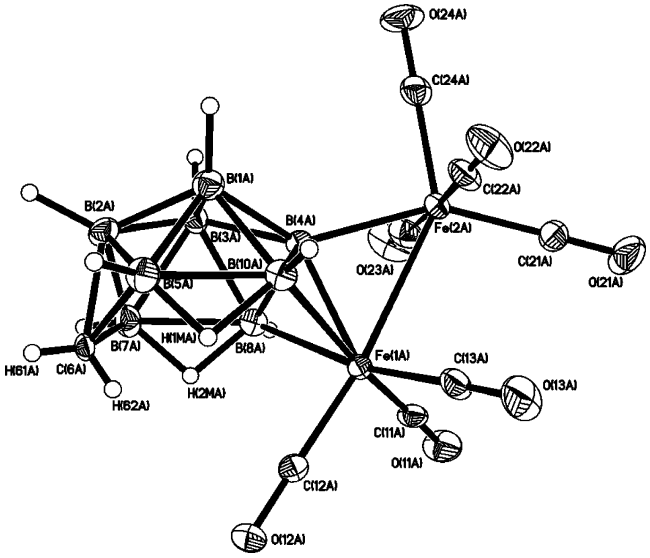

Figure 1. Structure of one of the three crystallographically independent anions of compound **3** showing the crystallographic labeling scheme; the other two anions are essentially identical. In this and subsequent figures, thermal ellipsoids are drawn with 40% probability Selected distances (Å) and angles (deg) are Fe(1A)−Fe(2A), 2.7033(6); Fe(1A)−B(4A), 1.996(3); Fe(1A)−B(8A), 2.205(3); Fe(1A)−B(10A), 2.213(3); Fe(1A)−C(11A), 1.789(3); Fe(1A)−C(12A), 1.761(3); Fe(1A)-C(13A), 1.779(3); Fe(2A)−B(4A), 2.140(3); Fe(2A)−C(21A), 1.810(3); Fe(2A)-C(22A), 1.803(3); Fe(2A)−C(23A), 1.799(3); Fe(2A)−C(24A), 1.773(3); B(4A)−Fe(1A)−Fe(2A), 51.54(9); B(8A)−Fe(1A)−Fe(2A), 83.25(8); B(10A)−Fe(1A)−Fe(2A), 82.80(8); B(4A)−Fe(2A)−Fe(1A), 46.92(8); Fe(1A)−B(4A)−Fe(2A), 81.54(11).

Data characterizing compound **3** are listed in Tables 1−3. Its IR spectrum shows four CO bands between 2055 and 1916 cm^{-1}, while its ^{11}B NMR spectrum contains a 1:1:2:2:2 set of resonances, consistent with the molecular mirror symmetry seen in the solid state. One of these resonances, at δ 61.4, remains a singlet upon retention of proton coupling and may be assigned to the *B*−Fe nucleus.[13] Attempts to substitute the Fe-bonded CO groups by other donor mol-

Chart 2

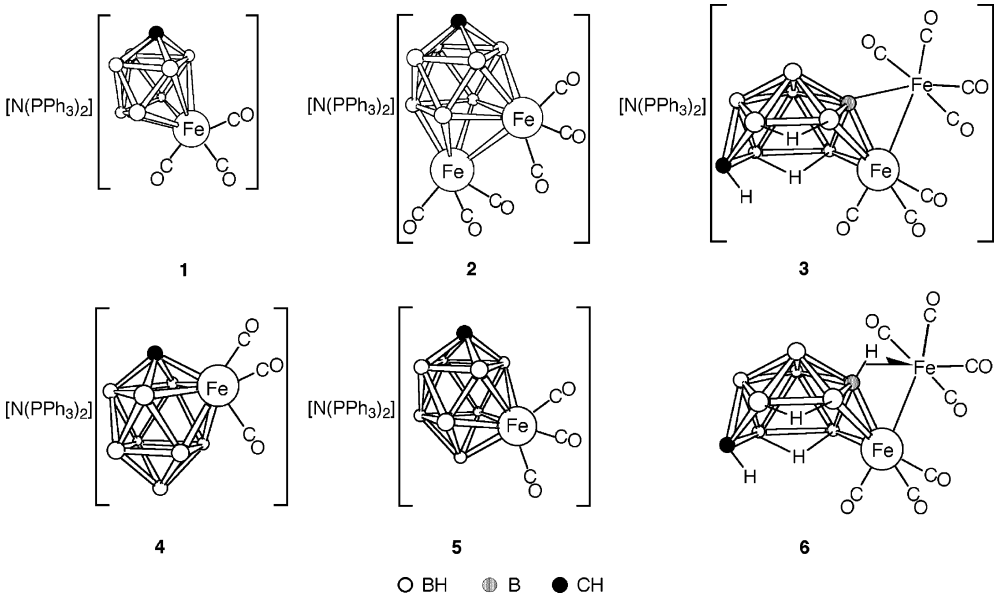

Table 1. Analytical and Physical Data

compd	color	yield (%)	IR ν_{max}(CO)[a] (cm^{-1})	anal.[b] C	H	N
$[N(PPh_3)_2][4,9\text{-}\{Fe(CO)_4\}\text{-}9,9,9\text{-}(CO)_3\text{-}arachno\text{-}9,6\text{-}FeCB_8H_{11}]$ (**3**)	yellow	47	2055 s, 1986 s, 1946 m, 1916 m	55.1 (55.3)	4.1 (4.3)	1.6 (1.5)
$[N(PPh_3)_2][2,2,2\text{-}(CO)_3\text{-}closo\text{-}2,1\text{-}FeCB_8H_9]$ (**4**)	yellow	79	2053 s, 1985 s	59.9 (59.9)[c]	5.0 (4.9)	1.7 (1.7)
$[N(PPh_3)_2][6,6,6\text{-}(CO)_3\text{-}closo\text{-}6,1\text{-}FeCB_8H_9]$ (**5**)	yellow	40	2033 s, 1964 s	61.0 (61.1)	5.2 (5.0)	1.8 (1.8)
$[4,9\text{-}\{Fe(CO)_4\}\text{-}4\text{-}(\mu\text{-}H)\text{-}9,9,9\text{-}(CO)_3\text{-}arachno\text{-}9,6\text{-}FeCB_8H_{11}]$ (**6**)	yellow	73	2121 m, 2063 s, 2046 s, 2027 w, 1985 w, 1967 w	22.8 (23.0)	2.7 (2.9)	
$[1,3,4,9\text{-}\{CuFe(CO)_4(PPh_3)\}\text{-}1,3\text{-}(\mu\text{-}H)_2\text{-}9,9,9\text{-}(CO)_3\text{-}arachno\text{-}9,6\text{-}FeCB_8H_9]$ (**7**)	orange	87	2075 s, 2023 s, 2005 s, 1972 w, 1950 w	41.3 (41.2)[c]	3.6 (3.5)	
$[1,3,4,9\text{-}\{AgFe(CO)_4(PPh_3)\}\text{-}1,3\text{-}(\mu\text{-}H)_2\text{-}9,9,9\text{-}(CO)_3\text{-}arachno\text{-}9,6\text{-}FeCB_8H_9]$ (**8**)	orange	82	2071 s, 2021 s, 2002 s, 1971 w, 1950 w	39.4 (39.7)	3.3 (3.3)	
$[4,9\text{-}(PEt_3)_2\text{-}9,9\text{-}(CO)_2\text{-}nido\text{-}9,6\text{-}FeCB_8H_{10}]$ (**9**)	pink	44	2008 s, 1960 s	39.0 (39.4)	8.4 (8.8)	

[a] Measured in CH_2Cl_2; in addition, the spectra of all compounds show a broad, medium-intensity band at ca. 2500−2550 cm^{-1} due to B−H absorptions. [b] Calculated values are given in parentheses. [c] Crystallizes with 0.25 equiv of CH_2Cl_2.

Table 2. ^1H and ^{13}C NMR Data[a]

compd	^1H[b] (δ)	^{13}C[c] (δ)
3	7.75−7.43 (m, 30H, Ph), 0.61 (br s, 1H, cage CH), 0.46 (br s, 1H, cage CH), −3.22 (br, 2H, B−H−B)	216.9 (CO), 215.6 (CO), 133.7−126.5 (Ph), 30.6 (br, cage C)
4	7.66−7.47 (m, 30H, Ph), 5.79 (br s, 1H, cage CH)	210.6 (CO), 134.0−126.5 (Ph), 76.2 (br, cage C)
5	7.68−7.43 (m, 30H, Ph), 5.10 (br s, 1H, cage CH)	214.0 (CO), 133.7−126.4 (Ph), 67.8 (br, cage C)
6	0.91 (br s, 1H, cage CH), 0.42 (br s, 1H, cage CH), −3.11 (br, 2H, B−H−B), −10.25 (q, J(BH) = 67, 1H, B−H ⇀ Fe)	211.6 (CO), 211.4 (CO), 207.0 (2 × CO), 202.4 (2 × CO), 198.3 (CO), 14.0 (br, cage C)
7	7.75−7.49 (m, 15H, Ph), 1.03 (br s, 1H, cage CH), 0.94 (br s, 1H, cage CH), −3.42 (br, 2H, B−H−B)	214.3 (CO), 212.2 (CO), 133.7−129.2 (Ph), 44.4 (br, cage C)
8	7.72−7.41 (m, 15H, Ph), 1.18 (br s, 1H, cage CH), 1.02 (br s, 1H, cage CH), −3.02 (br, 2H, B−H−B)	212.2 (CO), 209.8 (CO), 133.8−129.3 (Ph), 30.6 (br, cage C)
9	6.00 (br s, 1H, cage CH), 1.72 (m, 6H, PCH_2), 1.48 (m, 6H, PCH_2), 1.16 (m, 9H, CH_3), 0.55 (m, 9H, CH_3), −11.38 (q, J(BH) = 50, 2H, B−H ⇀ Fe)	214.0 (d, J(PC) = 30, CO), 107.9 (br, cage C), 19.5 (d, J(PC) = 29, PCH_2), 14.6 (d, J(PC) = 42, PCH_2), 7.0 (br, PCH_2CH_3), 6.3 (br, PCH_2CH_3)

[a] Chemical shifts (δ) in ppm, coupling constants (J) in Hz, measurements taken at ambient temperatures in CD_2Cl_2. [b] Resonances for terminal BH protons occur as broad unresolved signals in the range δ ca. −1 to +3. [c] ^1H-decoupled chemical shifts are positive to high frequency of $SiMe_4$.

Table 3. ^{11}B and ^{31}P NMR Data[a]

compd	^{11}B[b] (δ)	^{31}P[c] (δ)
3	61.4 (B(4)), 4.8, −6.6 (2B), −13.6 (2B), −30.7 (2B)	
4	37.1, 7.6, −3.0 (2B), −18.3 (2B), −28.8 (2B)	
5	61.9, −3.8 (3B), −24.7 (2B), −27.7 (2B)	
6	36.7 (B(4), J(HB) = 67), 7.0, −3.6 (2B), −14.7 (2B), −29.4 (2B)	
7	49.0 (B(4)), 6.1, −1.9 (2B), −17.0 (2B), −35.1 (2B)	5.8 (br)
8	53.1 (B(4)), 5.8, −3.3 (2B), −15.6 (2B), −32.5 (2B)	13.8 (vbr d, J(AgP) ≈ 555, $AgPPh_3$)
9	5.4 (2B), 2.7 (2B), 1.2 (2B), −8.5, −22.7 (d, J(PB) ≈ 134, B−PEt_3)	57.9 (s, $FePEt_3$), 7.2 (q, J(BP) ≈ 132, B−PEt_3)

[a] Chemical shifts (δ) in ppm, coupling constants (J) in Hz, measurements taken at ambient temperatures in CD_2Cl_2. [b] ^1H-decoupled chemical shifts are positive to high frequency of $BF_3{\cdot}Et_2O$ (external); resonances are of unit integral except where indicated. [c] ^1H-decoupled chemical shifts are positive to high frequency of 85% H_3PO_4 (external). Compounds **3**−**5** show an additional singlet at δ 21.7 for the $[N(PPh_3)_2]^+$ cation.

ecules failed, even in the presence of Me_3NO. In this respect, the anion of **3** displays similar chemical behavior to both **1** and **2**.[12]

Other 10-vertex metallaheteroboranes with the cluster formulation {*arachno*-9,6-MEB_8} (E = C, N, O, S, Se) are also known, with the majority (as here) formed by addition of the metal center to a preformed open-cage heteroborane.[14] However, the synthesis of compound **3** may also appropriately be compared with the formation of neutral, *arachno*-10-vertex nickel− and platinum−dicarbollide derivatives reported approximately three decades ago from reaction of the nine-vertex carboranes 4,6-R_2-*arachno*-4,6-$C_2B_7H_{11}$ (R = H, Me) with zero-valent nickel or platinum reagents.[15] In all three of the latter systems, incorporation of the metal vertex (Ni, Pt, Fe) into the cluster may be viewed as an oxidative insertion, with the ultimate products all having an arachno geometry and with the metal center in the three-connected 9-position in the cage.

Compound **3**, upon dissolution in toluene and heating to reflux temperature for 4 h, yielded the closed 10-vertex species $[N(PPh_3)_2][2,2,2\text{-}(CO)_3\text{-}closo\text{-}2,1\text{-}FeCB_8H_9]$ (**4**) as the only metallacarborane product. Formally, the reaction appears straightforward, with the four electrons available from the arachno → closo conversion utilized in the evolution of 1 equiv of H_2 by reduction of two formerly bridging protons and in the reductive loss of the former *exo*-$\{Fe(CO)_4\}^{2+}$ moiety as Fe(0). The precise details of the reaction, of course, may be more complex. The $^{11}B\{^1H\}$ NMR spectrum of **4** showed a 1:1:2:2:2 set of resonances, all of which showed coupling with terminal hydrogens in a fully coupled ^{11}B spectrum, confirming the loss of the exo-polyhedral iron unit. Other data for compound **4** (Tables 1−3) are straightforward.

In contrast with the thermal closure of **3** to give **4**, it was subsequently found that the carborane $[closo\text{-}4\text{-}CB_8H_9]^-$ and $[Fe_3(CO)_{12}]$ react in THF under reflux to form the anion $[6,6,6\text{-}(CO)_3\text{-}closo\text{-}6,1\text{-}FeCB_8H_9]^-$ via an oxidative insertion

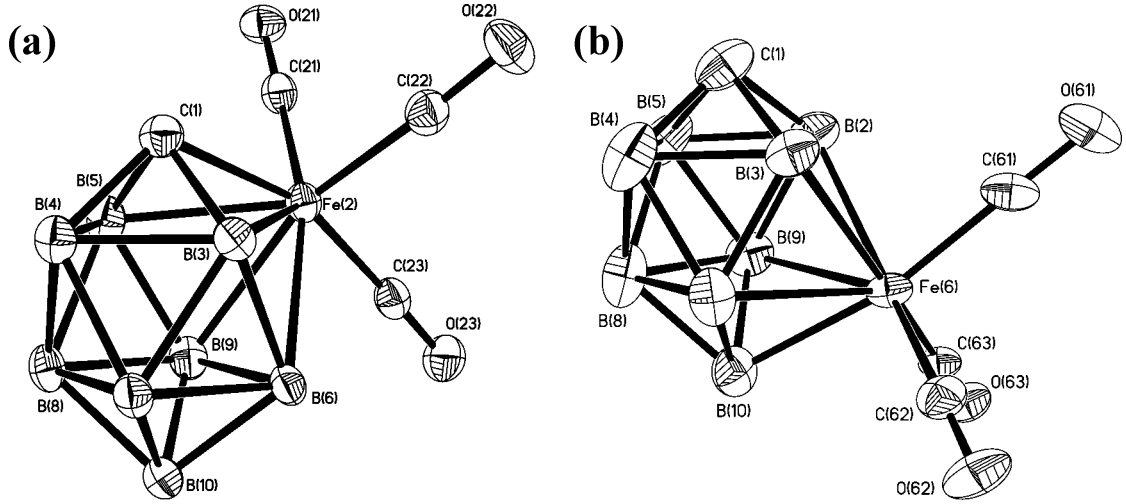

Figure 2. Structure of the anions of (a) compound **4** and (b) compound **5**, showing their crystallographic labeling schemes. For clarity, hydrogen atoms are omitted. Selected internuclear distances (Å) are as follows. For **4**: Fe(2)−C(1), 1.992(3); Fe(2)−B(3), 2.205(3); Fe(2)−B(5), 2.201(3); Fe(2)−B(6), 2.221(3); Fe(2)−B(9), 2.208(3); Fe(2)−C(21), 1.780(3); Fe(2)−C(22), 1.787(3); Fe(2)−C(23), 1.777(3). For **5**: B(2)···B(3), 2.044(6); Fe(6)−B(2), 2.210(4); Fe(6)−B(3), 2.185(4); Fe(6)−B(7), 2.221(4); Fe(6)−B(9), 2.270(4); Fe(6)−B(10), 2.073(4); Fe(6)−C(61), 1.770(4); Fe(6)−C(62), 1.779(4); Fe(6)−C(63), 1.772(3).

of the iron moiety. This anion was isolated as its $[N(PPh_3)_2]^+$ salt (**5**) following addition of $[N(PPh_3)_2]Cl$. The reaction whereby **5** is formed is analogous to the formation of **1** from [*closo*-1-CB_7H_8]$^-$ and $[Fe_3(CO)_{12}]$.[12] We note in passing that the anion of **5** is also obtained (albeit in poor yield and with considerable contamination) from [*nido*-1-CB_8H_{12}] and $[Fe_3(CO)_{12}]$. This is unsurprising as {*arachno*-4-CB_8} species are converted quite readily to their {*nido*-1-CB_8} counterparts upon heating.[6−8]

The $^{11}B\{^1H\}$ NMR spectrum for **5** is quite similar to that of its isomer **4** and shows a 1:3:2:2 set of resonances, all of which likewise become doublets upon retention of proton coupling. It may be of significance that the CO stretching frequencies for **5** are some 20 cm^{-1} lower than the ones for **4**, perhaps a reflection of the differing donor properties toward the iron vertex of CB_4 (**4**) versus B_5 (**5**) faces of the different {*nido*-CB_8} ligands in the two compounds. This phenomenon is readily understood (at least qualitatively) by consideration of the different electronegativities of boron versus carbon. Other spectroscopic data for **5** (Tables 1−3) are uncomplicated.

X-ray diffraction experiments were required to initially and definitively establish the structures of the ferracarborane anions of compounds **4** and **5**, in particular the relative positions of the carbon and iron vertexes. Given the C_s symmetry implied by the ^{11}B NMR data and with the ^1H NMR data showing only a single cage CH and the absence of any B−H−B protons, a closed-cage structure was likely, with only 2,1- or 6,1-{$FeCB_8$} isomers possible. This reasonably assumes that carbon will occupy a four-connected site[16] and that iron will be in the higher, five-connected one;[17] otherwise, 1,2- or 1,6-{$FeCB_8$} isomers would also be conceivable. The results of the structural studies are shown in Figure 2 and merit little further comment, save to note that in both cases the carbon and iron vertexes do indeed occupy four- and five-coordinate sites, as expected.[16,17] A (presumably unfavorable) {*closo*-10,1-$FeCB_8$} isomer is not observed. Perhaps surprisingly, we also found no evidence of isomerization of either **4** or **5** upon prolonged heating in refluxing toluene.

Although metallacarboranes with a {*closo*-MCB_8} architecture are known,[10b,18] they are relatively rare. These are limited primarily to clusters with 2,1- and 6,1-MCB_8 atom arrangements; we are aware of only one example[18a,b,f] with a {10,1-MCB_8} architecture. Moreover, the structurally characterized isomeric pair **4** and **5** is particularly interesting, and it will be important in the future to compare their respective reactivities.

(12) Franken, A.; McGrath, T. D.; Stone, F. G. A. *Organometallics* **2005**, *24*, 5157.
(13) Brew, S. A.; Stone, F. G. A. *Adv. Organomet. Chem.* **1993**, *35*, 135.
(14) Jones, J. H.; Stíbr, B.; Kennedy, J. D.; Thornton-Pett, M. *Inorg. Chim. Acta* **1994**, *227*, 163. Hilty, T. K.; Thompson, D. A.; Butler, W. M.; Rudolph, R. W. *Inorg. Chem.* **1979**, *18*, 2642. Alcock, N. A.; Jasztal, M. J.; Wallbridge, M. G. H. *J. Chem. Soc., Dalton Trans.* **1987**, 2793. Faridoon; Dhubhghaill, O. N.; Spalding, T. R.; Ferguson, G.; Kaitner, B.; Fontaine, X. L. R.; Kennedy, J. D. *J. Chem. Soc., Dalton Trans.* **1989**, 1657. Fontaine, X. L. R.; Kennedy, J. D.; Thornton-Pett, M.; Nestor, K.; Stíbr, B.; Jelínek, T.; Base, K. *J. Chem. Soc., Dalton Trans.* **1990**, 2887. Stíbr, B.; Jelínek, T.; Kennedy, J. D.; Fontaine, X. L. R.; Thornton-Pett, M. *J. Chem. Soc., Dalton Trans.* **1993**, 1261. Kim, Y.-H.; Brownless, A.; Cooke, P. A.; Greatrex, R.; Kennedy, J. D.; Thornton-Pett, M. *Inorg. Chem. Commun.* **1998**, *1*, 19.
(15) Green, M.; Howard, J. A. K.; Spencer, J. L.; Stone, F. G. A. *J. Chem. Soc., Dalton Trans.* **1975**, 2274.
(16) (a) Williams, R. E. *Adv. Inorg. Chem. Radiochem.* **1976**, *18*, 67. (b) Ott, J. J.; Gimarc, B. M. *J. Am. Chem. Soc.* **1986**, *108*, 4303.
(17) For example: Miller, V. R.; Sneddon, L. G.; Beer, D. C.; Grimes, R. N. *J. Am. Chem. Soc.* **1974**, *96*, 3090.
(18) (a) Salentine, C. G.; Rietz, R. R.; Hawthorne, M. F. *Inorg. Chem.* **1974**, *13*, 3025. (b) Stíbr, B.; Janousek, Z.; Base, K.; Dolansky, J.; Hermánek, S.; Solntsev, K. A.; Butman, L. A.; Kuznetsov, I. I.; Kuznetsov, N. T. *Polyhedron* **1982**, *1*, 831. (c) Crooke, J. E.; Greenwood, N. N.; Kennedy, J. D.; McDonald, W. S. *J. Chem. Soc., Chem. Commun.* **1983**, 83. (d) Solntsev, K. A.; Butman, L. A.; Kuznetsov, I. I.; Kuznetsov, N. T.; Stíbr, B.; Janousek, Z.; Base, K. *Koord. Khim.* **1983**, *9*, 993. (e) Alcock, N. W.; Taylor, J. G.; Wallbridge, M. G. H. *J. Chem. Soc., Chem. Commun.* **1983**, 1168. (f) Stíbr, B.; Janousek, Z.; Base, K.; Plesek, J.; Hermánek, S.; Solntsev, K. A.; Butman, L. A.; Kuznetsov, I. I.; Kuznetsov, N. T. *Collect. Czech. Chem. Commun.* **1984**, *49*, 1660. See also: Carr, M. J.; Franken, A.; Kennedy, J. D. *Dalton Trans.* **2004**, 2612.

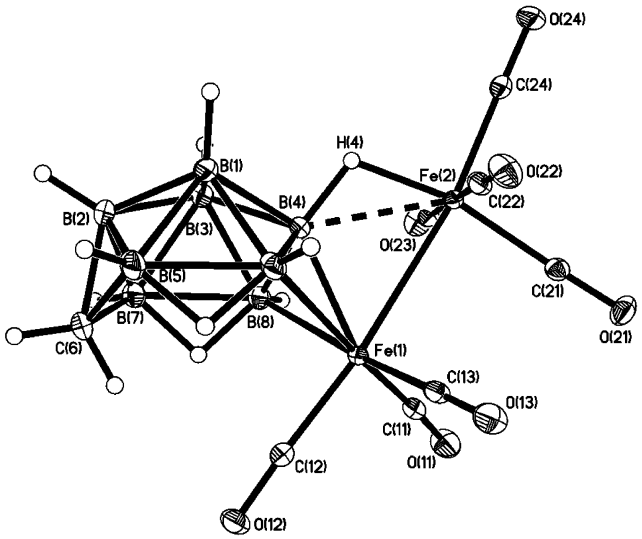

Figure 3. Structure of compound **6** showing the crystallographic labeling scheme. Selected distances (Å) and angles (deg) are Fe(1)−Fe(2), 2.6885(2); Fe(1)−B(4), 2.0213(11); Fe(1)−B(8), 2.2387(11); Fe(1)−B(10), 2.2573(12); Fe(1)−C(11), 1.8015(11); Fe(1)−C(12), 1.7742(10); Fe(1)−C(13), 1.7916(10); Fe(2)···B(4), 2.2923(11); Fe(2)−H(4), 1.592(13); B(4)−H(4), 1.245(13); Fe(2)−C(21), 1.8192(11); Fe(2)−C(22), 1.8313(10); Fe(2)−C(23), 1.8420(10); Fe(2)−C(24), 1.8226(10); B(4)−Fe(1)−Fe(2), 56.12(3); B(8)−Fe(1)−Fe(2), 85.52(3); B(10)−Fe(1)−Fe(2), 85.17(3); B(4)−Fe(2)−Fe(1), 47.06(3); Fe(1)−B(4)−Fe(2), 76.83(4).

Mention was made earlier of the difficulty of substituting the iron-bound CO groups in **3**. In an attempt to make these ligands more susceptible to replacement, we attempted to convert the anion of **3** to a neutral, zwitterionic species following a typical protocol, namely abstraction of a boron-bound hydride (using H^+) in the presence of a donor solvent.[2] Although an apparently neutral species was obtained, preliminary ^{1}H NMR evidence showed no donor molecule to be present and the same product was obtained regardless of the donor chosen. Ultimately, the identity of this product was established as the complex [4,9-{Fe(CO)$_4$}-4-(μ-H)-9,9,9-(CO)$_3$-*arachno*-9,6-FeCB$_8$H$_{11}$] (**6**). This was readily and cleanly obtained by protonation of **3** with CF_3SO_3H in CH_2Cl_2, and its precise nature was confirmed by an X-ray diffraction study (Figure 3).

The overall constitution of the starting compound **3** is seen to have been retained. As in the anion of the precursor, two iron atoms are connected via an Fe−Fe bond (Fe(1)−Fe(2) = 2.6885(2) Å), this being slightly shorter than in the parent. The exo-polyhedral iron unit (Fe(2)) is again bonded to a boron atom (B(4)) adjacent to the cage iron vertex (Fe(1)), but the Fe(2)···B(4) distance (2.2923(11) Å) is much longer than that in **3**. This is due to the presence of a hydrido ligand bridging this connectivity. Thus, a B−Fe σ bond in **3** has been protonated to form a B−H ⇀ Fe three-center, two-electron agostic-type linkage. This process is readily reversible upon treatment of **6** with even mild bases to regenerate the anion of **3**. The introduction or removal of a B···H···M bridging hydride (as here) by protonation or deprotonation at a {B···M} site has been observed previously.[19]

The NMR data for **6** (Tables 2 and 3) are in complete agreement with the structure established in the solid state. In the ^{1}H NMR spectrum, a diagnostic[13] broad quartet resonance of unit integral is seen at δ −10.25 (J(BH) = 67 Hz) and is assigned to the B−H ⇀ Fe linkage, and a further signal at δ −3.11 of relative intensity of 2 is in the region characteristic for B−H−B bridging hydrogens. The presence of a mirror plane of symmetry through C(6), B(2), B(4), Fe(1), Fe(2), and the midpoint of the B(1)−B(3) bond is reflected in the observed ^{11}B{^{1}H} NMR spectrum, the latter showing a 1:1:2:2:2 set of resonances, with one resonance at δ 36.7 showing only a relatively small J(HB) value of 67 Hz in a fully coupled ^{11}B NMR spectrum, again characteristic of the B−H ⇀ Fe bond.

Since the groups {M(PPh$_3$)}$^+$ (M = Cu, Ag) are isolobal with the proton,[20] it seemed likely that these cations would also react with the anion of **3**, in this case to afford trimetallic species. Accordingly, **3** was dissolved in CH_2Cl_2 and treated with 1 equiv of {M(PPh$_3$)}$^+$ (from [CuCl(PPh$_3$)]$_4$/Tl[PF$_6$] or Ag[PF$_6$]/PPh$_3$). These reactions yielded the compounds [1,3,4,9-{MFe(CO)$_4$(PPh$_3$)}-1,3-(μ-H)$_2$-9,9,9-(CO)$_3$-*arachno*-9,6-FeCB$_8$H$_9$] (M = Cu (**7**), Ag (**8**)), whose structures were definitively established by X-ray diffraction studies. The structure of compound **7** and geometric data for both **7** and **8** are presented in Figure 4. The two compounds gave isomorphous crystals and, as expected, are essentially isostructural, with some slight differences in geometric parameters arising merely as a result of the differing radii of Cu versus Ag. In both species, there is the same arrangement of iron atoms with Fe(1)−Fe(2) = 2.7543(4) Å in **7** and 2.7485(5) Å in **8**. As in the starting anion of **3**, the iron atom Fe(1) that is a cluster vertex is coordinated by three CO molecules and the exo-polyhedral Fe(2) center bears four such groups. The appended {M(PPh$_3$)} moiety is attached to the {*arachno*-FeCB$_8$} framework in a site that is distant from the open CBBFeBB face. Thus, the metal center M is bonded to Fe(2) (Fe(2)−Cu(1) = 2.5655(4) Å; Fe(2)−Ag(1) 2.6755(4) Å) and also approaches B(4), so that this boron is in contact with all three metal atoms (for **7**: Fe(1)−B(4) = 1.9937(15) Å, Fe(2)−B(4) = 2.2018(15), B(4)···Cu(1) = 2.2082(15) Å; for **8**: Fe(1)−B(4) = 1.9881(19) Å, Fe(2)−B(4) = 2.245(2) Å, B(4)···Ag(1) = 2.4876(19) Å). The *exo*-{M(PPh$_3$)} unit is further supported by interactions with the {BH(1)} and {BH(3)} vertexes, which partake in weak B−H ⇀ M three-center, two-electron bonds (for **7**: B(1)···Cu(1) = 2.4474(15) Å, B(3)···Cu(1) = 2.3309(15) Å; for **8**: B(1)···Ag(1) = 2.753(2) Å, B(3)···Ag(1) = 2.624(2) Å). Although in both **7** and **8**, the interaction with {BH(3)} is significantly stronger than that with {BH(1)}, both of these B···M distances are nevertheless rather long.

Spectroscopic data for compounds **7** and **8** (Tables 1−3) are consistent with their solid-state structures. Their ^{1}H NMR spectra display broad signals for the two B−H−B bridging hydrogens at δ −3.42 (**7**) and −3.02 (**8**), but no peaks were

(19) Examples include: (a) Vites, J.; Housecroft, C. E.; Eigenbrot, C.; Buhl, M. L.; Long, G. J.; Fehlner, T. P. *J. Am. Chem. Soc.* **1986**, *108*, 3304. (b) Ellis, D. D.; Jelliss, P. A.; Stone, F. G. A. *J. Chem. Soc., Dalton Trans.* **2000**, 2113. (c) Yasue, T.; Kawano, Y.; Shimoi, M. *Angew. Chem., Int. Ed.* **2003**, *42*, 1727.

(20) Stone, F. G. A. *Angew. Chem., Int. Ed. Engl.* **1984**, *23*, 89.

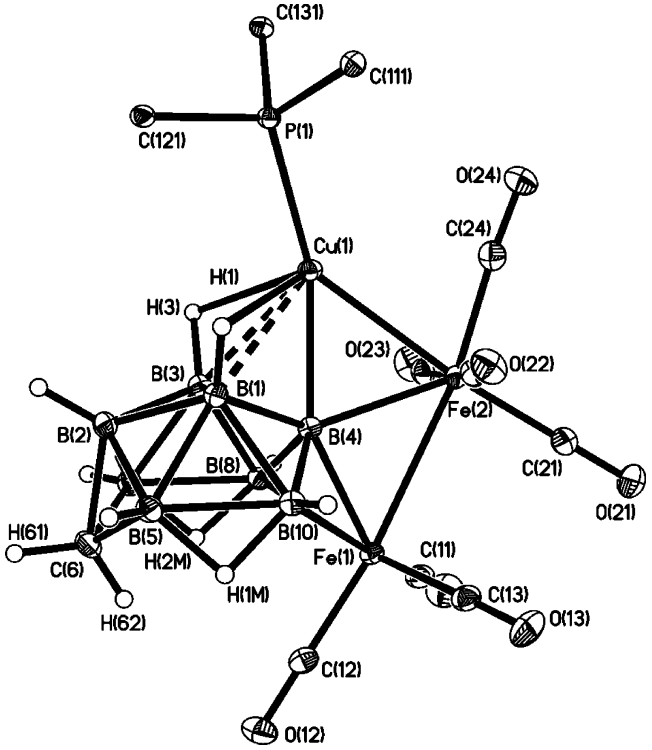

Figure 4. Structure of compound **7** showing the crystallographic labeling scheme; that of compound **8** is very similar. For clarity, all but the ipso carbons of phenyl rings are omitted. Selected distances (Å) and angles (deg) are as follows. For **7**: Fe(1)−Fe(2), 2.7543(4); Fe(1)−B(4), 1.9937(15); Fe(1)−B(8), 2.2304(17); Fe(1)−B(10), 2.2376(17); Fe(2)−Cu(1), 2.5655(4); Fe(2)−B(4), 2.2018(15); B(1)···Cu(1), 2.4474(15); B(3)···Cu(1), 2.3309(15); B(4)···Cu(1), 2.2082(15); B(4)−Fe(1)−Fe(2), 52.32(4); B(4)−Fe(2)−Cu(1), 54.54(4); B(4)−Fe(2)−Fe(1), 45.78(4); Cu(1)−Fe(2)−Fe(1), 100.269(10); Fe(1)−B(4)−Fe(2), 81.90(6); Fe(1)−B(4)−Cu(1), 152.87(8); Fe(2)−B(4)−Cu(1), 71.15(5). For **8**: Fe(1)−Fe(2), 2.7485(5); Fe(1)−B(4), 1.9881(19); Fe(1)−B(8), 2.228(2); Fe(1)−B(10), 2.226(2); Fe(2)−Ag(1), 2.6755(4); Fe(2)−B(4), 2.245(2); B(1)···Ag(1), 2.753(2); B(3)···Ag(1), 2.624(2); B(4)···Ag(1), 2.4876(19); C(24)···Ag(1), 2.699(2); B(4)−Fe(1)−Fe(2), 53.73(6); B(4)−Fe(2)−Ag(1), 59.98(5); B(4)−Fe(2)−Fe(1), 45.55(5); Ag(1)−Fe(2)−Fe(1), 105.444(12); Fe(1)−B(4)−Fe(2), 80.72(7); Fe(1)−B(4)−Ag(1), 149.11(10); Fe(2)−B(4)−Ag(1), 68.63(5).

observed that could be assigned to the agostic B−H ⇀ Mbridges. The absence of the latter signals is not unusual and results from solution dynamic processes that are rapid on the NMR time scale, even at low temperature.[21] The boron atom (B(4)) that is in contact with all three of the metal atoms gives rise to a rather deshielded signal at δ 49.0 (**7**) and 53.1 (**8**) in the respective $^{11}B\{^1H\}$ NMR spectra, this peak remaining a singlet upon retention of proton coupling. Other signals in the NMR spectra are in characteristic positions and need not be discussed further, save to note that the $^{31}P\{^1H\}$ NMR spectrum for **7** shows a broad resonance at δ 5.8 that is broadened by unresolved coupling to the adjacent copper and boron nuclei, while the corresponding signal for **8** occurs as a broad doublet (J(AgP) ≈ 555 Hz) centered at δ 13.8 for which individual ^{107}Ag− and ^{109}Ag−^{31}P couplings could not be resolved.

Chart 3

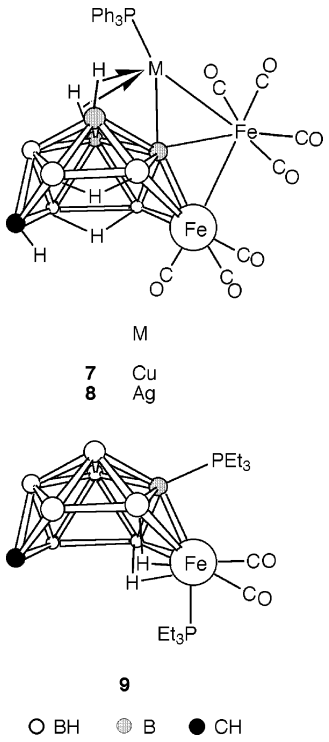

Despite the fact that compound **6** was prepared with a view to replacing its CO groups with other donor ligands, this proved difficult. With a number of reagents, the only process that occurred appeared to be decomposition—often via loss of the exo-polyhedral iron center. However, with strong donors, some products could be isolated. Thus, although no reaction occurred on stirring **6** with PEt_3, upon addition of excess Me_3NO to the reaction mixture, the pink monoiron species [4,9-$(PEt_3)_2$-9,9-$(CO)_2$-*nido*-9,6-$FeCB_8H_{10}$] (**9**) was formed.

The $^{11}B\{^1H\}$ NMR spectrum of **9** indicated a mirror symmetric structure with five resonances of relative intensity 2:2:2:1:1 (high to low frequency), in sharp contrast with the 1:1:2:2:2 pattern seen for **3** (and **6**−**8**). This reversal of the intensity pattern was suggestive of a change in cluster character from arachno to nido, and is seen in other arachno- versus nido-10-vertex clusters, such as the $\{C_2B_8\}$, $\{CB_9\}$, $\{SB_9\}$, and $\{B_{10}\}$ systems.[8,22] For **9**, the highest field ^{11}B signal (δ −22.7) is a doublet that has characteristic coupling of J(PB) = 134 Hz and arises from PEt_3 substitution at one boron atom. A corresponding quartet signal appears in the $^{31}P\{^1H\}$ NMR spectrum at δ 7.2 with J(BP) = 132 Hz plus a singlet at δ 57.9 that is assigned to an Fe-bound PEt_3 moiety. The presence of this phosphine at the metal center results in the sole signal for CO ligands being a doublet (δ 214.0; J(PC) = 30 Hz) in the $^{13}C\{^1H\}$ NMR spectrum. Since no other signals for carbonyl ligands were found, it seemed likely that the exo-polyhedral iron unit had been lost and it was reasonably proposed that the boron-bound phosphine

(21) (a) Jeffrey, J. C.; Ruiz, M. A.; Sherwood, P.; Stone, F. G. A. *J. Chem. Soc., Dalton Trans.* **1989**, 1845. (b) Carr, N.; Gimeno, M. C.; Goldberg, J. E.; Pilotti, M. U.; Stone, F. G. A.; Topaloglu, I. *J. Chem. Soc., Dalton Trans.* **1990**, 2253. (c) Jeffery, J. C.; Jelliss, P. A.; Stone, F. G. A. *J. Chem. Soc., Dalton Trans.* **1993**, 1073. (d) Jeffery, J. C.; Jelliss, P. A.; Rees, L. H.; Stone, F. G. A. *Organometallics* **1998**, *17*, 2258.

(22) Beckett, M. A.; Kennedy, J. D. *J. Chem. Soc., Chem. Commun.* **1983**, 575. Bown, M.; Fontaine, X. L. R.; Kennedy, J. D. *J. Chem. Soc., Dalton Trans.* **1988**, 1467. See also: Hermánek, S. *Chem. Rev.* **1992**, *92*, 325 and references therein.

had become attached at B(4). This last proposal is also consistent with the observed retention of mirror symmetry, as B(2) is the only other boron that lies on the mirror plane. In the ^{1}H NMR spectrum, multiplet signals for the ethyl protons of the two different PEt_3 ligands are evident, along with only a single cage CH resonance at δ 6.00 of unit relative intensity. There is also a broad, integral-2 quartet to high field (δ −11.38; J(BH) = 50 Hz) that is suggestive of B−H−Fe bridges, which one would expect to be located between the Fe center and the adjacent boron vertexes (B(8) and B(10)). Such hydrogen atoms, bridging the cluster 8,9 and 9,10 connectivities, plus the absence of an endo hydrogen on the carbon vertex are also typical of the nido structure that the ^{11}B NMR data suggests. In contrast, the 5,10- and 7,8-bridging hydrogens in **3**, along with the endo hydrogen on the cage carbon atom, are characteristic of arachno-10-vertex clusters.

Although the structure of **9** was evident from the NMR spectral data, crystals of **9** suitable for study by X-ray diffraction were grown to confirm the proposed architecture. The result of this experiment is shown in Figure 5. Although the crystals were only of modest quality, the above formulation of **9** was verified unequivocally. The central {9,6-$FeCB_8$} cage is seen to have been retained, with substitution by PEt_3 moieties at iron and at boron (Fe(1)−P(1) = 2.216(2) Å; B(4)−P(2) = 1.890(8) Å) and loss of the second iron fragment. The Fe(1)−B(8) (2.178(8) Å) and Fe(1)−B(10) (2.188(9) Å) bonds are bridged by hydrido ligands (H(89) and H(91), respectively) as expected, the siting of these hydrogens being consistent with the NMR data and with the proposed nido character of the cluster. This is further corroborated by the B(5)−B(10) and B(7)−B(8) bond lengths in **9**, 1.941(12) and 1.945(11) Å, respectively, which are rather longer than the corresponding distances (typically 1.876(5) and 1.880(5) Å, respectively, for one of the crystallographically independent anions) in **3**. This elongation is well established as typical of nido-10-vertex clusters. The arachno → nido conversion involved in the formation of **9** may be viewed as a simple oxidation of the cluster, possibly effected by the presence of excess Me_3NO or alternatively by the reductive loss of the formerly exo-polyhedral iron fragment, formally Fe(II), as Fe(0).

In contrast with the above reaction of **6** with PEt_3 in the presence of Me_3NO, a preliminary investigation of the reaction of **6** with $CNBu^t$ and Me_3NO suggests that the product(s) retain an arachno-10-vertex character and that the exo-polyhedral iron center is still present. However, yields in this system are very low and products with various multiple degrees of substitution are evident, making separation very difficult. Notably, though, it appears that substitution occurs exclusively at the exo iron atom. We hope to report more upon this system in the future.

Conclusion

Several new 10-vertex ferracarboranes have been prepared starting from 8-boron-atom substrates, and their reactivity has been studied. The carborane [*arachno*-4-CB_8H_{14}] adds two iron fragments upon heating with [$Fe_3(CO)_{12}$]: one as a vertex and the second in an exo-polyhedral site, giving the anion of compound **3**. The latter upon thermolysis undergoes a cage-closure reaction to afford the anion of **4**, whereas the isomeric anion in **5** is produced by direct iron insertion into [*closo*-4-CB_8H_9]$^-$ in its reaction with [$Fe_3(CO)_{12}$]. The isomeric pair **4** and **5** themselves represent useful starting substrates for which a comparative reactivity study will be of interest, bearing in mind their isolobal relationship with [$Mn(CO)_3(\eta$-$C_5H_5)$].[23] They should also provide useful comparisons with the {CB_7} derivatives **1** and **2** and with the corresponding 12-vertex {$FeCB_{10}$} system.[24−26] Moreover, compound **3** contains both Fe−Fe and Fe−B linkages to the exo-polyhedral iron, and upon protonation, it is the Fe−B σ-bond that is attacked, converting it cleanly to a B−H → Fe agostic-type bridge.

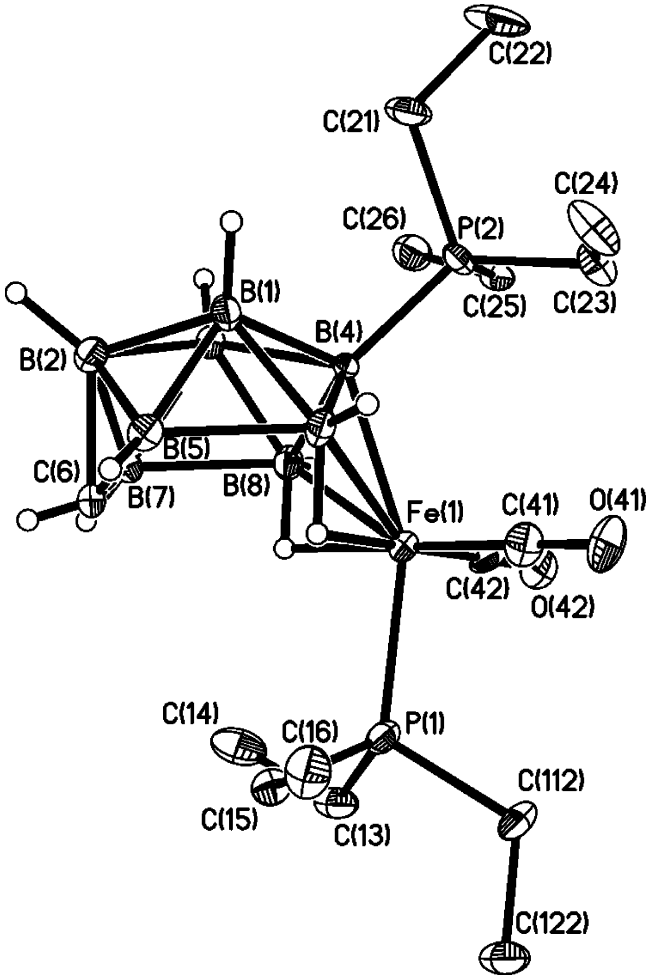

Figure 5. Structure of one of the crystallographically independent molecules of compound **9** showing the crystallographic labeling scheme. For clarity, only the major component of the disordered Et group is shown and ethyl hydrogens are omitted. Selected distances (Å) and angles (deg) are as follows. Fe(1)−P(1), 2.216(2); Fe(1)−C(41), 1.769(8); Fe(1)−C(42), 1.758(8); Fe(1)−H(89), 1.59(4); B(8)−H(89), 1.19(2); Fe(1)−H(91) 1.57-(4); B(10)−H(91), 1.20(2); B(4)−Fe(1), 2.209(8); B(8)−Fe(1), 2.178(8); B(10)−Fe(1), 2.188(9); B(4)−P(2), 1.890(8); B(4)−Fe(1)−P(1), 156.1(2); B(8)−Fe(1)−P(1), 115.8(2); B(10)−Fe(1)−P(1), 120.2(2); C(41)−Fe(1)−P(1), 92.7(3); C(42)−Fe(1)−P(1), 92.1(2); P(2)−B(4)−Fe(1), 116.6(4).

(23) Hata, M.; Kautz, J. A.; Lu, X. L.; McGrath, T. D.; Stone, F. G. A. *Organometallics* **2004**, *23*, 3590.

Experimental Section

General Considerations. All reactions were carried out under an atmosphere of dry, oxygen-free dinitrogen using standard Schlenk line techniques. Solvents were stored over and distilled from appropriate drying agents under dinitrogen prior to use. Petroleum ether refers to that fraction of boiling point 40−60 °C. Chromatography columns (typically ca. 15 cm in length and ca. 2 cm in diameter) were packed with silica gel (Acros, 60−200 mesh). NMR spectra were recorded at the following frequencies (MHz): ^{1}H, 360.1; ^{13}C, 90.6; ^{11}B, 115.5; and ^{31}P, 145.8. The compounds [*arachno*-4-CB_8H_{14}],[8] [NBu^n_4][*closo*-4-CB_8H_9],[8] and [CuCl-$(PPh_3)]_4$[27] were prepared according to the literature; all other materials were used as received.

Synthesis of [$N(PPh_3)_2$][4,9-{$Fe(CO)_4$}-9,9,9-$(CO)_3$-*arachno*-9,6-$FeCB_8H_{11}$]. The compounds [$Fe_3(CO)_{12}$] (0.50 g, 1.0 mmol) and [*arachno*-4-CB_8H_{14}] (0.056 g, 0.5 mmol) were dissolved in THF (10 mL) and heated to reflux for 24 h. The mixture was cooled to room temperature, and [$N(PPh_3)_2$]Cl (0.29 g, 0.5 mmol) was added. Solvent was removed in vacuo, and the residue was dissolved in CH_2Cl_2 (2 mL) and transferred to the top of a chromatography column. Elution with CH_2Cl_2−petroleum ether (4:1) gave a yellow fraction from which was obtained, after removal of solvent in vacuo and then crystallization from CH_2Cl_2−petroleum ether, yellow microcrystals of [$N(PPh_3)_2$][4,9-{$Fe(CO)_4$}-9,9,9-$(CO)_3$-*arachno*-9,6-$FeCB_8H_{11}$] (**3**; 0.23 g).

Synthesis of [$N(PPh_3)_2$][2,2,2-$(CO)_3$-*closo*-2,1-$FeCB_8H_9$]. Compound **3** (0.23 g, 0.25 mmol) was dissolved in toluene (10 mL) and heated to reflux for 4 h. Volatiles were removed in vacuo, and the residue was dissolved in CH_2Cl_2 (2 mL) and subjected to column chromatography. Elution with neat CH_2Cl_2 gave a yellow fraction. Removal of solvent in vacuo, followed by crystallization from CH_2Cl_2−petroleum ether, yielded yellow microcrystals of [$N(PPh_3)_2$]-[2,2,2-$(CO)_3$-*closo*-2,1-$FeCB_8H_9$] (**4**; 0.14 g).

Synthesis of [$N(PPh_3)_2$][6,6,6-$(CO)_3$-*closo*-6,1-$FeCB_8H_9$]. The compounds [$Fe_3(CO)_{12}$] (0.40 g, 0.79 mmol) and [NBu^n_4][*closo*-4-CB_8H_9] (ca. 0.18 g, 0.5 mmol) were heated to reflux in THF (10 mL) for 18 h. The mixture was then cooled to room temperature, and [$N(PPh_3)_2$]Cl (0.29 g, 0.5 mmol) was added. Solvent was removed in vacuo, and the residue was dissolved in CH_2Cl_2 (2 mL) and transferred to the top of a chromatography column. Elution with CH_2Cl_2 gave a pale yellow fraction. Removal of solvent in vacuo followed by crystallization from CH_2Cl_2−petroleum ether yielded yellow microcrystals of [$N(PPh_3)_2$][6,6,6-$(CO)_3$-*closo*-6,1-$FeCB_8H_9$] (**5**; 0.16 g).

Synthesis of [4,9-{$Fe(CO)_4$}-4-(μ-H)-9,9,9-$(CO)_3$-*arachno*-9,6-$FeCB_8H_{11}$]. Compound **3** (0.23 g, 0.25 mmol) was dissolved in CH_2Cl_2 (10 mL), CF_3SO_3H (0.25 mL) was added, and the mixture was stirred at room temperature for 30 min. After filtration through Celite, the filtrate was evaporated in vacuo. The residue was dissolved in CH_2Cl_2 (2 mL) and transferred to the top of a chromatography column. Elution with CH_2Cl_2−petroleum ether (1:1) gave a yellow fraction from which removal of solvent in vacuo followed by crystallization from CH_2Cl_2−petroleum ether afforded yellow microcrystals of [4,9-{$Fe(CO)_4$}-4-(μ-H)-9,9,9-$(CO)_3$-*arachno*-9,6-$FeCB_8H_{11}$] (**6**; 0.080 g).

Synthesis of [1,3,4,9-{$MFe(CO)_4(PPh_3)$}-1,3-(μ-H)$_2$-9,9,9-$(CO)_3$-*arachno*-9,6-$FeCB_8H_9$]. (i) Compound **3** (0.23 g, 0.25 mmol), [$CuCl(PPh_3)]_4$ (0.09 g, 0.06 mmol), and Tl[PF_6] (0.09 g, 0.25 mmol) were stirred in CH_2Cl_2 (10 mL) at room temperature for ca. 18 h. The resulting mixture was filtered through Celite, and the filtrate was evaporated to dryness in vacuo. The residue was taken up in CH_2Cl_2 (2 mL) and applied to a chromatography column. Elution with CH_2Cl_2−petroleum ether (1:1) gave an orange fraction that was collected, evaporated in vacuo, and crystallized from CH_2Cl_2−petroleum ether to give orange microcrystals of [1,3,4,9-{$CuFe(CO)_4(PPh_3)$}-1,3-(μ-H)$_2$-9,9,9-$(CO)_3$-*arachno*-9,6-$FeCB_8H_9$] (**7**; 0.16 g). (ii) Similarly, compound **3** (0.23 g, 0.25 mmol), Ag[PF_6] (0.070 g, 0.25 mmol), and PPh_3 (0.070 g, 0.25 mmol) yielded orange microcrystals of [1,3,4,9-{$AgFe(CO)_4$-(PPh_3)}-1,3-(μ-H)$_2$-9,9,9-$(CO)_3$-*arachno*-9,6-$FeCB_8H_9$] (**8**; 0.16 g).

Synthesis of [4,9-$(PEt_3)_2$-9,9-$(CO)_2$-*nido*-9,6-$FeCB_8H_{10}$]. Compound **6** (0.10 g, 0.25 mmol) was dissolved in CH_2Cl_2 (10 mL), PEt_3 (0.25 mL, 0.20 g, 1.69 mmol) and Me_3NO (0.075 g, 1.0 mmol) were added, and the mixture was stirred at room temperature for ca. 5 days. Volatiles were removed under reduced pressure, and the residue was redissolved in CH_2Cl_2 (2 mL) and transferred to the top of a chromatography column. Elution with CH_2Cl_2−petroleum ether (4:1) gave a pink fraction from which removal of solvent in vacuo and crystallization from Et_2O (−30 °C) yielded red microcrystals of [4,9-$(PEt_3)_2$-9,9-$(CO)_2$-*nido*-9,6-$FeCB_8H_{10}$] (**9**; 0.050 g).

Structure Determinations. Diffraction-quality crystals of compounds **3**−**5** were obtained by slow diffusion of petroleum ether into CH_2Cl_2 solutions at −30 °C; those of **6** and **9** were grown by slow cooling of saturated hexane solutions to −30 °C, while those of **7** and **8** were grown similarly from pentane solutions at the same temperature. Experimental data for compounds **3**−**9** are reported in Table 4. Diffraction data were acquired at 110(2) K using a Bruker−Nonius X8 Apex area-detector diffractometer (graphite-monochromated Mo Kα radiation, λ = 0.71073 Å). Several sets of data frames were collected at different θ values for various initial values of ϕ and ω, each frame covering a 0.5 increment in ϕ or ω. The data frames were integrated using SAINT;[28] the substantial redundancy in data allowed empirical absorption corrections (SADABS)[28] to be applied on the basis of multiple measurements of equivalent reflections.

The structures were solved (SHELXS-97) via conventional direct methods and—for all but **3**—were refined (SHELXL-97) by full-matrix least-squares on all F^2 data using SHELXTL.[28,29] All non-hydrogen atoms were assigned anisotropic displacement parameters. The locations of the cage carbon atoms were verified by examination of the appropriate internuclear distances and the magnitudes of their isotropic thermal displacement parameters. All of the hydrogen atoms in organic functions, plus terminal cluster H atoms in the structure of **9**, were set riding on their parent atoms in calculated positions; all other cluster H atoms were located in difference maps and allowed positional refinement—with the exception of the B−H−Fe bridging hydrogens in **9**, which could only be positionally refined subject to restraints (DFIX card in SHELXL with B−H 1.20(5) Å and Fe−H 1.60(5) Å). All hydrogen atoms were assigned fixed isotropic thermal parameters calculated as U_{iso}(H) = 1.2 × U_{iso}(parent), or U_{iso}(H) = 1.5 × U_{iso}(parent) for methyl hydrogens.

Crystals of **3** contained three formula units per asymmetric fraction, with the three independent units differing primarily in the

(24) Ellis, D. D.; Franken, A.; Jelliss, P. A.; Stone, F. G. A.; Yu, P.-Y. *Organometallics* **2000**, *19*, 1993.
(25) Ellis, D. D.; Franken, A.; Jelliss, P. A.; Kautz, J. A.; Stone, F. G. A.; Yu, P.-Y. *J. Chem. Soc., Dalton* Trans. **2000**, 2509.
(26) Franken, A.; Du, S.; Jelliss, P. A.; Kautz, J. A.; Stone, F. G. A. *Organometallics* **2001**, *20*, 1597.
(27) Jardine, F. H.; Rule, J.; Vohra, G. A. *J. Chem. Soc. A* **1970**, 238.
(28) *APEX 2*, version 1.0; Bruker AXS: Madison, WI, 2003−2004.
(29) *SHELXTL*, version 6.12; Bruker AXS: Madison, WI, 2001.

Table 4. Crystallographic Data for Compounds **3**−**9**

	3	**4**	**5**	**6**
formula	$C_{44}H_{41}B_8Fe_2NO_7P_2$	$C_{40}H_{39}B_8FeNO_3P_2$	$C_{40}H_{39}B_8FeNO_3P_2$	$C_8H_{12}B_8Fe_2O_7$
fw	955.90	785.99	785.99	418.36
space group	$P2_1/n$	$P\bar{1}$	$P2_1/n$	*Pbca*
a, Å	16.2454(12)	11.6121(6)	14.990(3)	11.8803(4)
b, Å	56.345(4)	11.7781(6)	14.936(3)	15.9624(7)
c, Å	16.3333(13)	14.4449(8)	17.660(4)	17.6111(7)
α, deg	90	80.587(2)	90	90
β, deg	113.414(4)	85.802(2)	94.854(10)	90
γ, deg	90	82.398(2)	90	90
V, Å^3	13719.6(18)	1929.19(18)	3939.7(14)	3339.7(2)
Z	12	2	4	8
ρ_{calc}, g cm^{-3}	1.388	1.353	1.325	1.664
μ (Mo Kα), mm^{-1}	0.755	0.515	0.504	1.763
reflns measured	144 940	37 290	32 351	36 420
indep reflns	35 715	11 184	9070	6392
R_{int}	0.0456	0.0398	0.0557	0.0273
wR2(all data), R1[a]	0.1105, 0.0524	0.1642, 0.0583	0.1301, 0.0581	0.0582, 0.0231
	7·C_5H_{12}	**8**·C_5H_{12}	**9**	
formula	$C_{31}H_{38}B_8CuFe_2O_7P$	$C_{31}H_{38}AgB_8Fe_2O_7P$	$C_{15}H_{40}B_8FeO_2P_2$	
fw	815.30	859.63	456.74	
space group	$P\bar{1}$	$P\bar{1}$	$P\bar{1}$	
a, Å	11.4290(14)	11.5823(17)	12.6993(14)	
b, Å	12.8599(17)	12.8429(19)	13.4499(16)	
c, Å	14.3117(18)	14.420(2)	15.9396(18)	
α, deg	96.175(6)	97.590(4)	114.448(5)	
β, deg	110.698(5)	112.387(4)	90.694(4)	
γ, deg	106.957(5)	104.934(4)	90.124(4)	
V, Å^3	1829.3(4)	1851.6(5)	2478.2(5)	
Z	2	2	4	
ρ_{calc}, g cm^{-3}	1.480	1.542	1.224	
μ (Mo Kα), mm^{-1}	1.447	1.384	0.747	
reflns measured	36 939	37 597	39 747	
indep reflns	11 143	12 108	11 168	
R_{int}	0.0309	0.0425	0.0724	
wR2(all data), R1[a]	0.0743, 0.0299	0.0739, 0.0318	0.2724, 0.1090	

[a] $wR2 = [\sum\{w(F_o^2 - F_c^2)^2\}/\sum w(F_o^2)^2]^{1/2}$; $R1 = \sum||F_o| - |F_c||/\sum|F_o|$ with $F_o > 4\sigma(F_o)$.

dispositions of the cations. The large number of data and parameters required refinement by blocked-matrix least-squares on F^2, with one cation and one anion per block (and some atoms common to two blocks), but the model was otherwise as described above.

For both **7** and **8**, one molecule of pentane as solvate co-crystallized in the asymmetric unit along with one molecule of the compound. In both cases, the solvate had two disordered methylene units, of which the two parts were assigned refining complementary occupancies, in the approximate ratios 60:40 (**7**) and 58:42 (**8**) at convergence. The geometries within the two parts of the solvate were restrained to be similar using the SAME card in SHELXL, but treatment was otherwise as above.

Two independent molecules were also found in the asymmetric fraction of crystals of **9** with the molecules differing in the site of a disordered ethyl group in the PEt_3 ligand bound to iron. In each case, the two parts were assigned refining complementary occupancies, with approximate ratios of 71:29 and 76:24 at convergence. The structure was otherwise refined as above.

Acknowledgment. We thank the Robert A. Welch Foundation for support. The Bruker X8 APEX diffractometer was purchased with funds received from the National Science Foundation Major Research Instrumentation Program (Grant No. CHE-0321214).

Supporting Information Available: Full details of the crystal structure analyses in CIF format. This material is available free of charge via the Internet at http://pubs.acs.org.

IC051946I